

CFD Models for Rivers and Sediment Transport

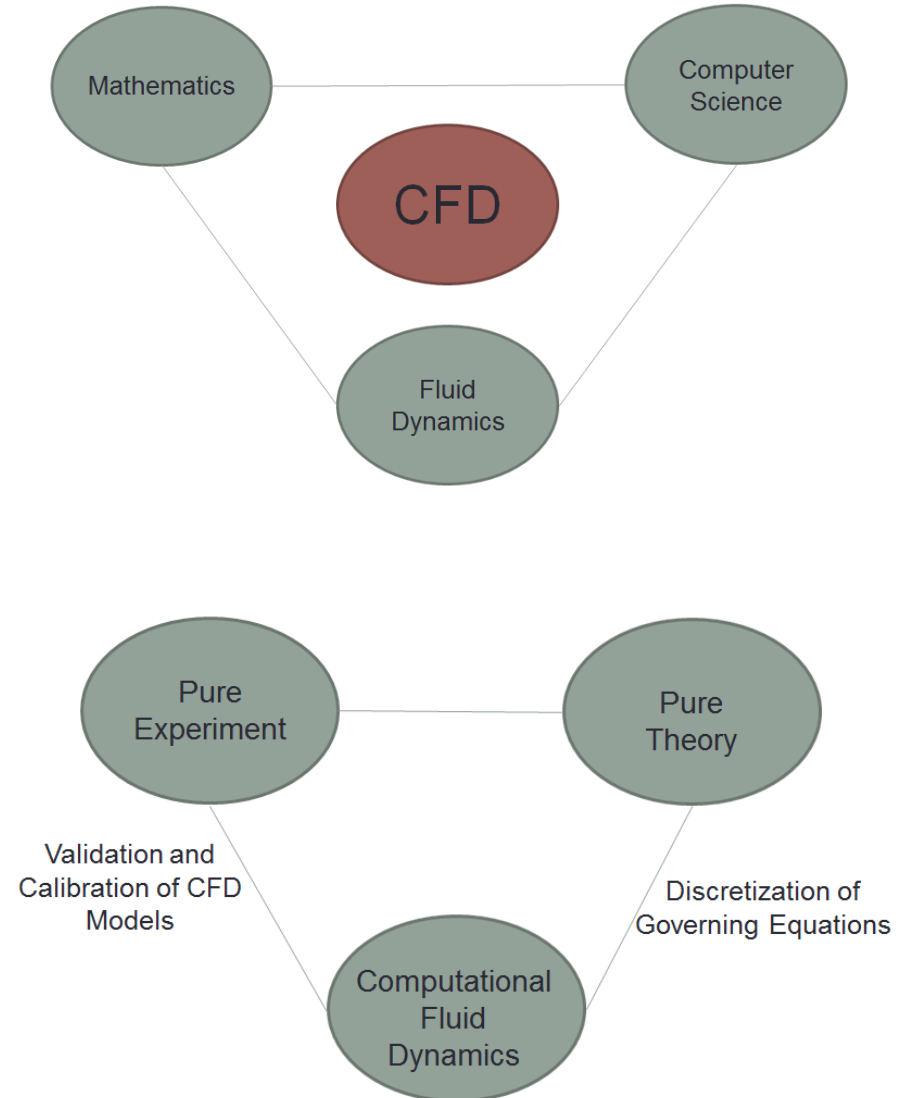
By Kennard Lai, Weimin Li and Yishu Zhang

4/28/2016

CIVE 717 - River Mechanics

What is CFD?

- Atmospheric Sciences
- Oceanography
- Mechanical Engineering
- Thermodynamics
- Aeronautical Engineering
- Environmental Engineering
- Geotechnical Engineering
- Biology
- Civil Engineering
 - River mechanics
 - Hydraulics
 - Structural Engineering



CFD versus Physical Experiments

- CFD is a numerical experiment
 - Some aspects of fluid flow, such as turbulence, can *only* be modeled with statistical results from physical experiments.
 - CFD can be more cost effective than physical modeling
 - CFD can be used to model physically impossible conditions, such as inviscid flow.
 - CFD is very valuable for modeling extreme conditions such as extremely high temperature or velocity which may be impossible to model physically.
 - Physical experiments must always be used to validate CFD codes
- 

CFD Software

- ANSYS
 - Commonly used in consulting and industry
 - Formerly called Fluent
 - Finite volume method



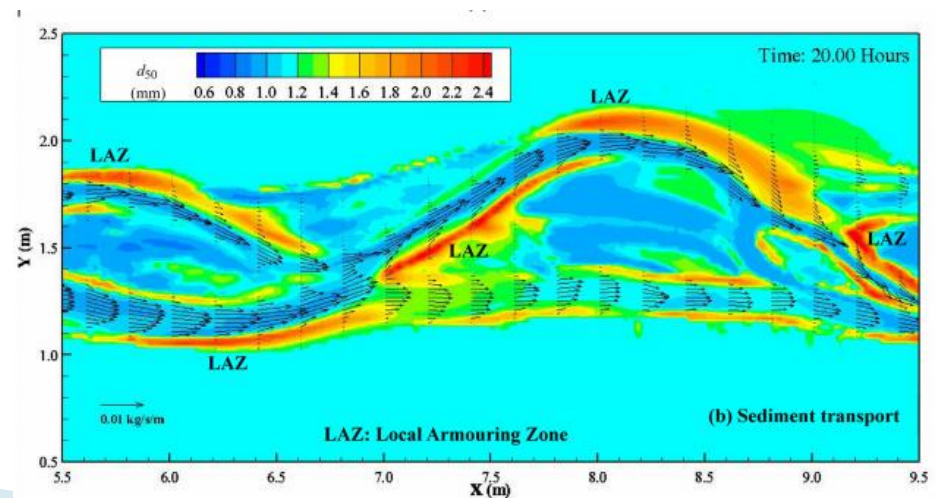
- COMSOL Multiphysics
 - Compatible with MATLAB
 - Physics modeling software
 - Finite element method



- Research Codes
 - MATLAB
 - FORTRAN
 - C
 - Etc.

Applications in Civil Engineering

- Sediment transport in rivers
- Sediment deposition in reservoirs
- Waves driven by wind shear on reservoir
- Detention time of chlorine in baffle tanks in water treatment facilities
- Modeling pollution plumes from off-shore fish farms
- Design of whitewater kayak parks



Numerical Model

- ▶ Reynolds-averaged Navier Stokes equations for incompressible, fully turbulent flow

Continuity: $\frac{dU_i}{dx_i} = 0$

Momentum: $\frac{\partial U_i}{\partial t} + U_i \frac{\partial U_i}{\partial x_i} = \frac{1}{\rho} \frac{1}{\partial x_i} (-P \delta_{ij} - \overline{\rho u_i' u_j'}) + \frac{f_i}{\rho}$

Where U is the velocity averaged over time t,

x is the spatial geometrical scale,

ρ is the density,

δ_{ij} is the Kronecker delta,

and u is the velocity fluctuation over time during one time step ∂t

$\overline{u_i' u_j'}$ is the turbulent stresses being modeled with the Boussinesq approximation

$$\overline{u_i' u_j'} = \nu_t \left(\frac{\partial U_i}{\partial x_j} + \frac{\partial U_j}{\partial x_i} \right) - \frac{2}{3} k \delta_{ij}$$

Where k is the turbulent kinetic energy term

Numerical Model

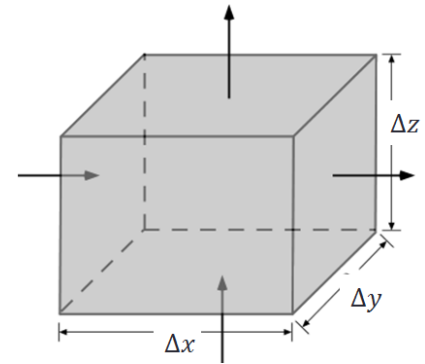
- Sediment transport model
 - Bed load transport
 - Sediment mass-balance equation
 - Suspended load transport
 - Convection-diffusion equation
 - Empirical Input
 - Near bed equilibrium concentration at a reference level
 - Equilibrium bed load transport
 - Non-equilibrium adaptation length

Grid Generation

- The governing equations are approximated over control volumes or a grid

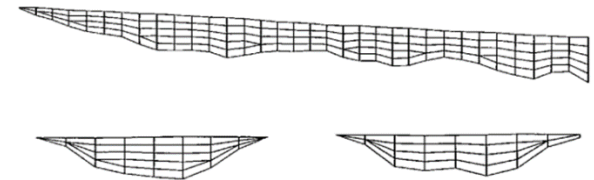
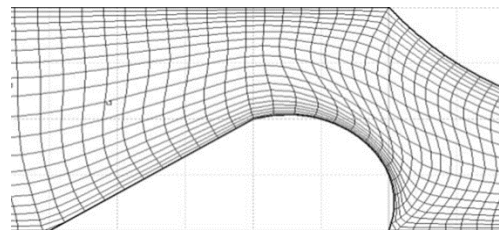
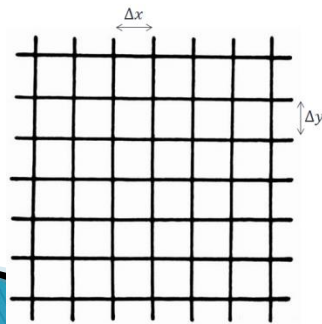
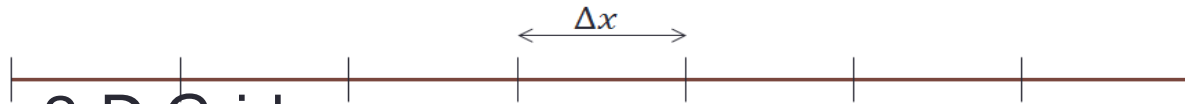
- 1-D Grid

- Water surface elevation model in hydraulics (standard step method)



- 2-D Grid

- Cartesian, structured, and unstructured

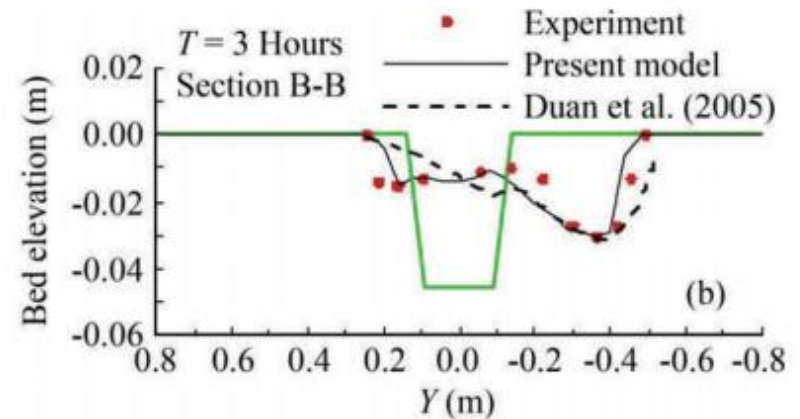
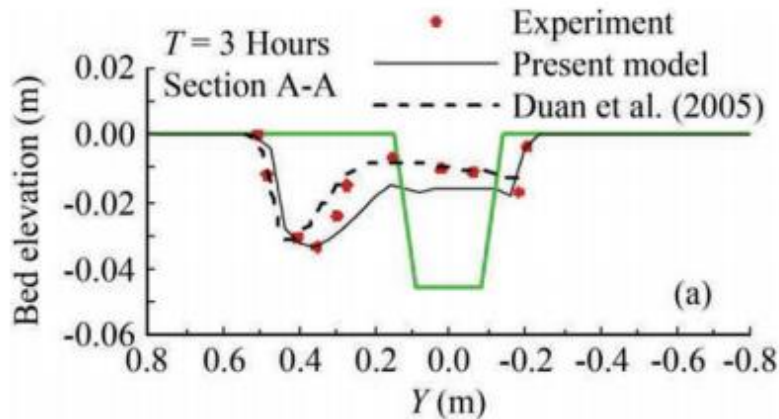


Grid Generation

- 3-D Grid
 - Three dimensional grids are very computationally expensive
 - Grid sizes are smaller in areas with high gradients to capture the range of motions and boost accuracy and efficiency
- Unstructured grids (most common)
- Coarse grid causes instabilities close to the boundary
 - Inflation
 - Changing shapes

Physical Validation

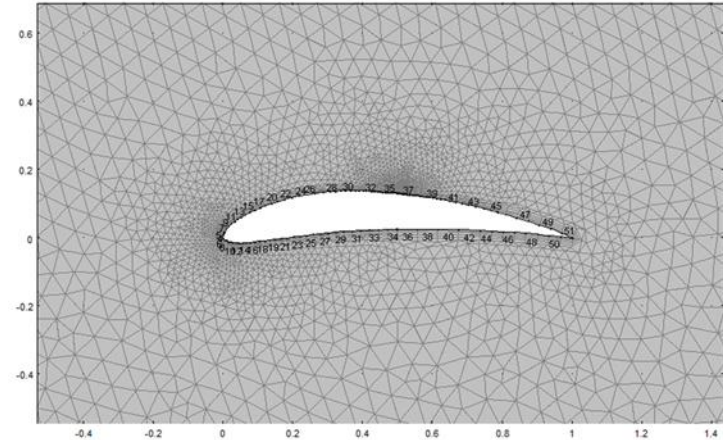
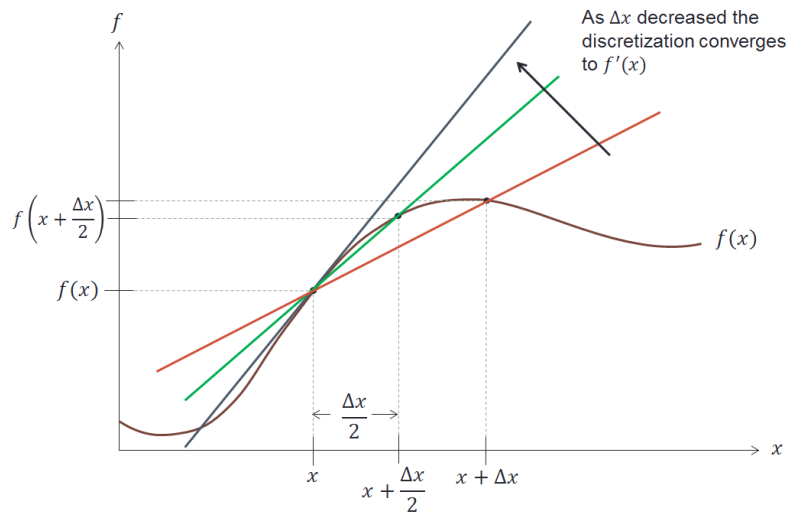
- Physical experiments must always be used to validate CFD codes



- Good agreement between model results and experiment results indicates the CFD code is accurate and correct.

Errors and limitation to consider in CFD

- Errors of $O(\Delta x)$ in discretization of equations
- Errors caused by using averaged parameters (Reynolds averaged Navier-Stokes)
- Numerical physics



Case Study I: 2D Depth-Averaged Flow Modeling with an Unstructured Hybrid Mesh (Lai 2010)

One dimensional (1D) flow models have been used for many years in hydraulic engineering. These 1D models remain useful, particularly for applications with long reaches, such as 50 km, or over a long time period, such as over a year.

However, there are situations where multidimensional modeling is needed. For example, modeling with 3D Navier-Stokes equations is necessary if flow around hydraulic structure is of interest. With increasing computational resources, 2D models are used for river projects. Examples of commercial or public-domain 2D codes are DHI, USACE, CCHE2D, TELEMAC, etc.

Governing Equations

Most open channel flows are relatively shallow. As a result of negligible vertical motions, the 3D Navier-Stokes equations are vertically averaged to obtain a set of depth-averaged 2D equations.

$$\frac{\partial h}{\partial t} + \frac{\partial(hU)}{\partial x} + \frac{\partial(hV)}{\partial y} = 0$$

$$\frac{\partial(hU)}{\partial t} + \frac{\partial(hUU)}{\partial x} + \frac{\partial(hVU)}{\partial y} = \frac{\partial(hT_{xx})}{\partial x} + \frac{\partial(hT_{xy})}{\partial y} - gh \frac{\partial z}{\partial x} - \frac{\tau_{bx}}{\rho}$$

$$\frac{\partial(hV)}{\partial t} + \frac{\partial(hUV)}{\partial x} + \frac{\partial(hVV)}{\partial y} = \frac{\partial(hT_{xy})}{\partial x} + \frac{\partial(hT_{yy})}{\partial y} - gh \frac{\partial z}{\partial y} - \frac{\tau_{by}}{\rho}$$

where x, y = horizontal Cartesian coordinates; t = time; h = water depth; U, V = depth-averaged velocity components in x and y directions, respectively; T_{xx}, T_{xy}, T_{yy} = depth-averaged stresses due to turbulence as well as dispersion; $z = z_b + h$ = water surface elevation; z_b = bed elevation; ρ = water density; τ_{bx}, τ_{by} = bed shear stresses

The bed stresses are obtained using the Manning resistance equation as

$$(\tau_{bx}, \tau_{by}) = \rho C_f \sqrt{U^2 + V^2} (U, V)$$

where $C_f = \frac{gn^2}{H^{1/3}}$; n = Manning's roughness coefficient; The depth-averaged stresses are calculated with the

(continued on next slide)

Case Study I: 2D Depth-Averaged Flow Modeling with an Unstructured Hybrid Mesh (Lai 2010)

Boussinesq's formulation as $T_{xx} = 2(\vartheta + \vartheta_t) \frac{\partial U}{\partial x}$,
 $T_{yy} = 2(\vartheta + \vartheta_t) \frac{\partial V}{\partial y}$, $T_{xy} = 2(\vartheta + \vartheta_t) \left(\frac{\partial U}{\partial y} + \frac{\partial V}{\partial x} \right)$ where
 ν = kinematic viscosity of water, and ν_t = eddy
 viscosity

The eddy viscosity is calculated with a turbulent
 model. Dr. Lai has used two models in his study,
 the depth-averaged parabolic model and the two-
 equation k - ϵ model. For the parabolic model, the
 eddy viscosity is calculated as

$$\vartheta_t = C_t U_* h$$

where C_t = the model constant with the range from
 0.3 to 1.0. A default value of 0.7 is used in Dr. Lai's
 study; $U_* = C_f^{1/2} \sqrt{U^2 + V^2}$

For the two-equation k - ϵ model, the eddy viscosity is calculated
 as $\vartheta_t = C_\mu k^2 / \epsilon$ with the two additional equations as following.

$$\begin{aligned} \frac{\partial(hk)}{\partial t} + \frac{\partial(hUk)}{\partial x} + \frac{\partial(hVk)}{\partial y} &= \frac{\partial}{\partial x} \left(\frac{h\vartheta_t}{\sigma_k} \frac{\partial k}{\partial x} \right) + \frac{\partial}{\partial y} \left(\frac{h\vartheta_t}{\sigma_k} \frac{\partial k}{\partial y} \right) + P_h + P_{kb} - h\epsilon \\ \frac{\partial(h\epsilon)}{\partial t} + \frac{\partial(hU\epsilon)}{\partial x} + \frac{\partial(hV\epsilon)}{\partial y} &= \frac{\partial}{\partial x} \left(\frac{h\vartheta_t}{\sigma_\epsilon} \frac{\partial \epsilon}{\partial x} \right) + \frac{\partial}{\partial y} \left(\frac{h\vartheta_t}{\sigma_\epsilon} \frac{\partial \epsilon}{\partial y} \right) + C_{\epsilon 1} \frac{\epsilon}{k} P_h + P_{\epsilon b} \\ &\quad - C_{\epsilon 2} h \frac{\epsilon^2}{k} \end{aligned}$$

Following Rodi's recommendation, one has

$$P_h = h\vartheta_t \left[2 \left(\frac{\partial U}{\partial x} \right)^2 + 2 \left(\frac{\partial V}{\partial y} \right)^2 + \left(\frac{\partial U}{\partial y} + \frac{\partial V}{\partial x} \right)^2 \right], P_{kb} = C_f^{-1/2} U_*^3,$$

$$P_{\epsilon b} = C_{\epsilon_r} C_{\epsilon 2} C_\mu^{-1/2} C_f^{-3/4} U_*^4 h, C_\mu = 0.09, C_{\epsilon 1} = 1.44, C_{\epsilon 2} = 1.92,$$

$$\sigma_k = 1,$$

$$\sigma_\epsilon = 1.3, C_{\epsilon_r} = 1.8 - 3.6$$

Case Study I: 2D Depth-Averaged Flow Modeling with an Unstructured Hybrid Mesh (Lai 2010)

Boundary Conditions

Boundary conditions consist of four types: inlet, exit, solid wall, and symmetry.

(1) Inlet: A total flow discharge, in the form of a constant or a time series hydrograph, is specified. Velocity distribution along the inlet is calculated in a way that the total discharge is satisfied. If a flow is subcritical at an inlet, however, the water surface elevation is not needed; instead a constant water surface slope normal to the inlet is assumed. If a flow is supercritical at the inlet, however, the water surface elevation at the inlet is needed as another input. If the k - ϵ model is used, the values of k and ϵ are also needed which, for most applications, have negligible impact on the flow pattern.

(2) Exit: Water surface elevation is specified at a subcritical exit but it is not required if flow at the exit is supercritical. Instead, it is assumed that the derivative of the water surface elevation normal to the exit is constant at the supercritical exit.

(3) Solid wall: no-slip condition is applied and the wall functions are employed. At a solid wall, $(\tau_{bx}, \tau_{by}) = \rho C_\mu^{1/4} k_p^{1/2} k(U, V) / \ln(Ey_p^+)$ where $y_p^+ = C_\mu^{1/4} k_p^{1/2} y_p / \nu$ for the k - ϵ model and k_p = turbulent kinetic energy at a mesh cell that contains the wall boundary; and $(\tau_{bx}, \tau_{by}) = \rho U_* k(U, V) / \ln(Ey_p^+)$ where $y_p^+ = U_* y_p / \nu$ for the depth-averaged parabolic model where k = von Karman constant, 0.41, y_p = normal distance from the center of a cell to a wall, and E = constant, 9.758.

(4) Symmetry: The normal velocity component is set to zero at a symmetry boundary.

Case Study I: 2D Depth-Averaged Flow Modeling with an Unstructured Hybrid Mesh (Lai 2010)

Discretization

The 2D depth-averaged may be written in tensor form as

$$\frac{\partial h}{\partial t} + \nabla \cdot (hV) = 0$$

$$\frac{\partial (hV)}{\partial t} + \nabla \cdot (hVV) = -gh\nabla z + \nabla \cdot (hT) - \frac{\tau_b}{\rho}$$

where V = velocity vector, T = second-order stress tensor, τ_b = bed shear stress vector

As an illustration, consider a generic convection-diffusion equation that is representative of all governing equations

$$\frac{\partial (h\Phi)}{\partial t} + \nabla \cdot (hV\Phi) = \nabla \cdot (\Gamma\nabla\Phi) + S_\Phi^*$$

where Φ = a dependent variable, a scalar or a component of a vector, Γ = diffusivity coefficient, S_Φ^* = source/sink term

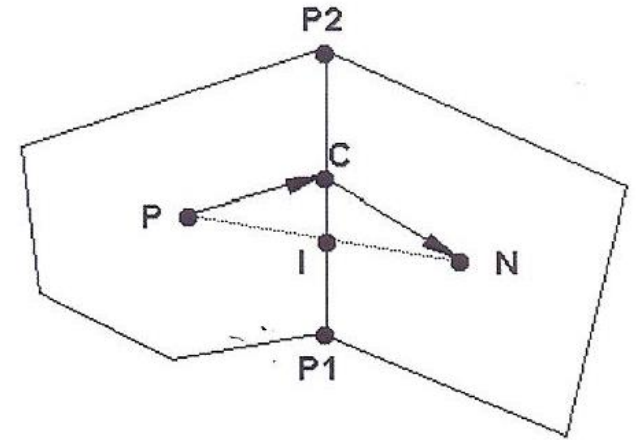


Figure 1 Schematic illustrating a polygon cell P along with one of its neighboring polygon N (after Dr. Lai)

Case Study I: 2D Depth-Averaged Flow Modeling with an Unstructured Hybrid Mesh (Lai 2010)

Integration over an arbitrarily shaped polygon P shown in the Figure 1 leads to

$$\begin{aligned} \frac{(h_p^{n+1}\phi_p^{n+1} - h_p^n\phi_p^n)A}{\Delta t} + \sum_{\text{all sides}} (h_c V_c |s|)^{n+1} \phi_c^{n+1} \\ = \sum_{\text{all sides}} (\Gamma_c^{n+1} \nabla \phi^{n+1} \cdot n|s|) + S_\phi \end{aligned}$$

where Δt = time step, A = cell area, $V_c = V_c \cdot n$ = velocity component normal to the polygonal side (e.g. P_1P_2 in the figure 1) and is evaluated at the side center C , n = unit normal vector of a polygon side, s = polygon side distance vector, and $S_\phi = S_\phi^* A$, subscript C indicates a value evaluated at the center of a polygon side and superscripts n or $n+1$ denotes the time level.

$$\nabla \phi \cdot n|s| = D_n(\phi_N - \phi_P) + D_c(\phi_{P2} - \phi_{P1})$$

$$D_n = \frac{s}{(r_1 + r_2) \cdot n}$$

$$D_c = \frac{(r_1 + r_2) \cdot s/|s|}{(r_1 + r_2) \cdot n}$$

The implicit solver requires the solution of nonsymmetric sparse matrix linear equations. In Dr. Lai's study, the standard conjugate gradient solver with ILU preconditioning is used.

Wetting and Drying Treatment

Most natural rivers consist of main and side channels, bars, inlands, and floodplains and the bed may be wet or dry depending on flow stage. The wetting-drying property is not known and is part of the solution. A robust wetting-drying algorithm, therefore, is needed. Such an algorithm offers the benefit that the same solution domain and mesh may be used for all flow discharges. A cell is wet if water depth is above 1.0 mm.

Case Study I: 2D Depth-Averaged Flow Modeling with an Unstructured Hybrid Mesh (Lai 2010)

Sandy River Delta Simulation

The SANDY River Delta dam is located near the confluence of the Sandy and Columbia rivers, east of Portland, Oregon (Figure 2). As a result of its closure in 1938, flow has been redirected from the east distributary to the west (downstream) distributary. Although it was once the main distributary channel, the east distributary is currently only activated under high flow conditions. New efforts to improve aquatic habitat conditions have considered the removal of the dam. This model was used to evaluate possible effects on the delta area if the dam is removed. The bed elevation contours of the study area are displayed in the Figure 2.

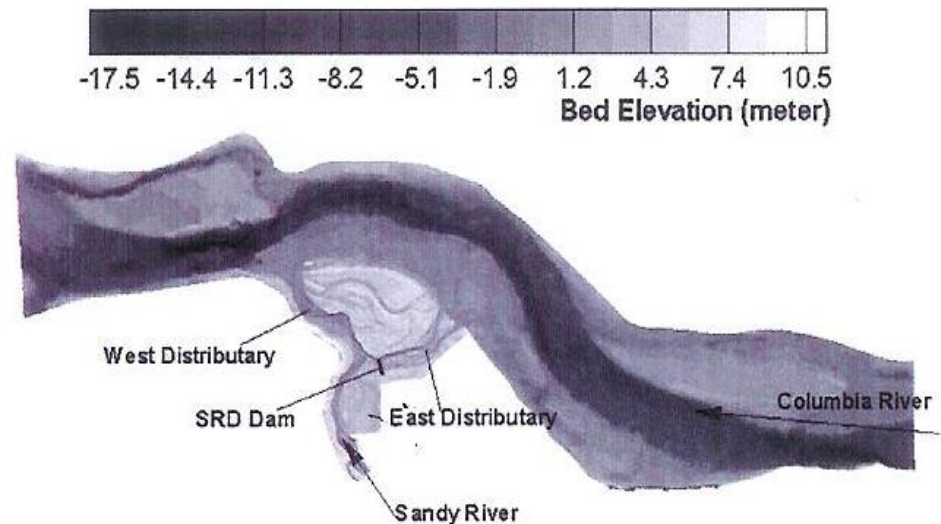


Figure 2 Study area of the Sandy and Columbia River confluence, along with the topography for the solution domain (after Dr. Lai)

Case Study I: 2D Depth-Averaged Flow Modeling with an Unstructured Hybrid Mesh (Lai 2010)

The solution domain was covered with a hybrid mesh with a total of 37,637 cells, A portion of the mesh around the delta is shown in the Figure 3.

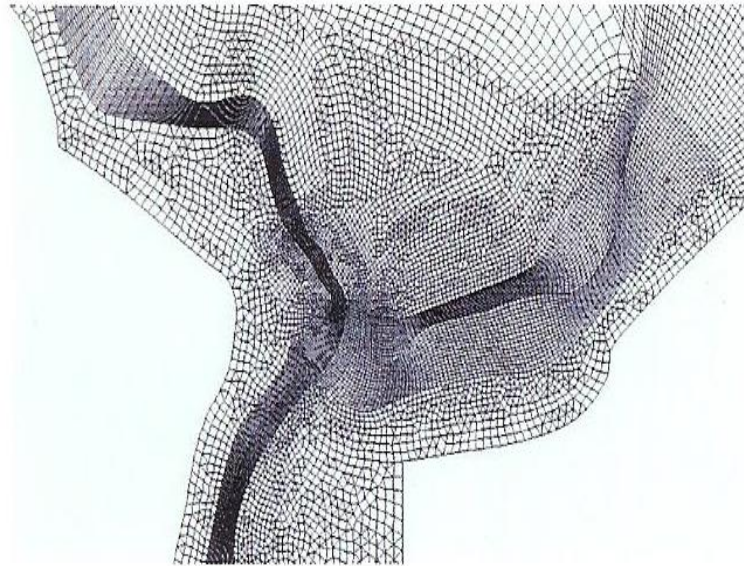


Figure 3 Portion of the mesh used to model the Sandy River and Columbia River Delta (after Dr. Lai)

Case Study I: 2D Depth-Averaged Flow Modeling with an Unstructured Hybrid Mesh (Lai 2010)

Flow resistance is a model input represented by the Manning's coefficient n . The solution domain was divided into a number of roughness zones based on the underlying bed properties, delineated using the available aerial photo and the bed gradation data. In the figure 14, the zones 1, 2, and 3 represent the main channel of the Sandy River; zones 4 and 5 represent the main channel of Columbia River; Zone 6 consists mostly of sand bars and less vegetated areas; and zone 7 represents islands and floodplains with heavy vegetation. The calibrated Manning's coefficients are tabulated in the Table 1.

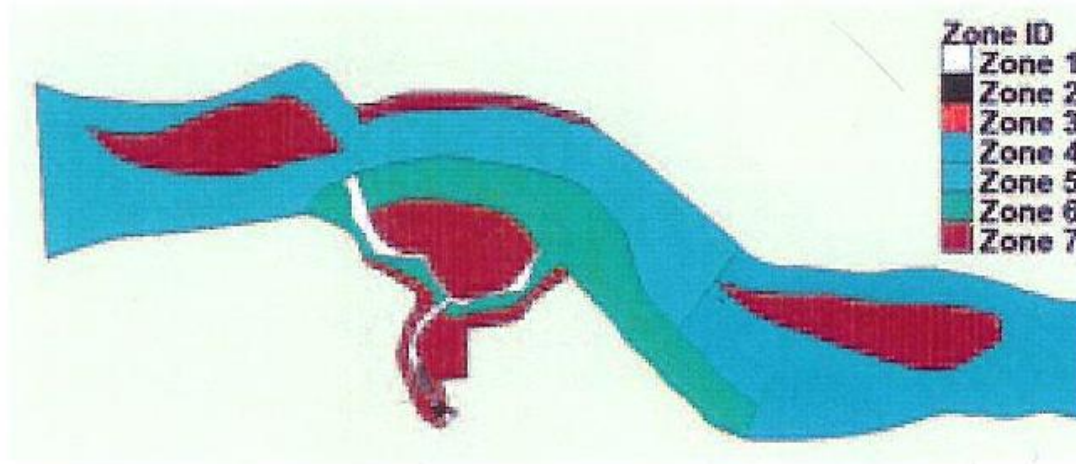


Figure 4 Roughness zones used for the Sandy River Delta (after Dr. Lai)

Table 1 Manning's coefficient for Different Zones shown in the Figure 4

Zone number	1	2	3	4	5	6	
Manning's n	0.035	0.06	0.15	0.035	0.035	0.035	0.06

Case Study I: 2D Depth-Averaged Flow Modeling with an Unstructured Hybrid Mesh (Lai 2010)

The simulated water surface elevation on the Sandy River is compared with the field data in the first following figure.

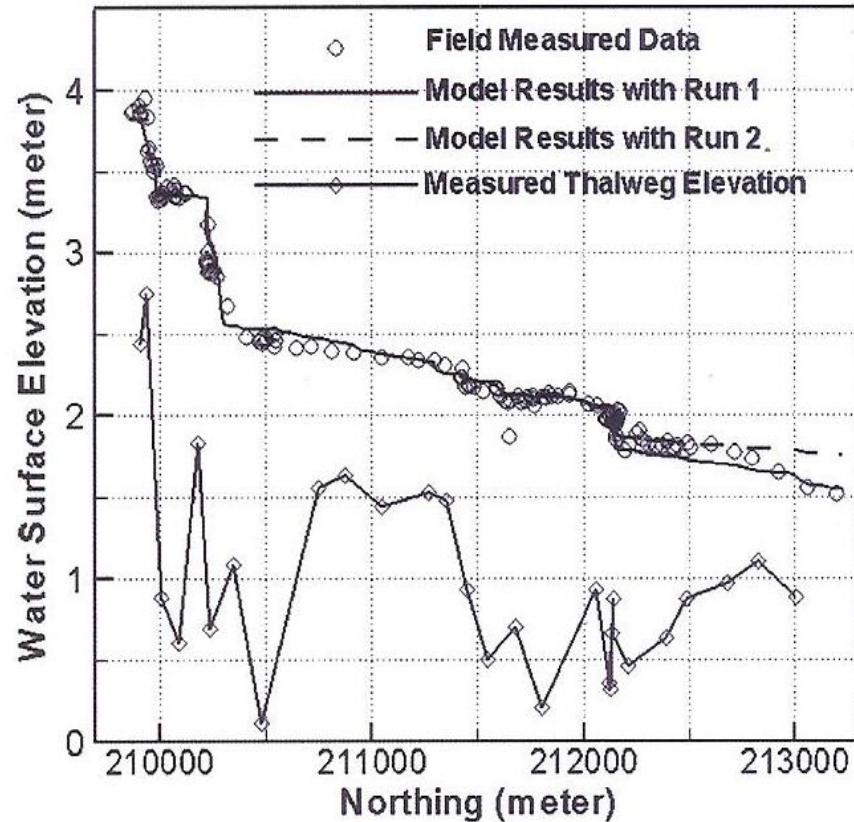


Figure 5 Comparison of field measured and model predicted water surface elevations for the October 12, 2005 flow conditions along Sandy River (after Dr. Lai)

Case Study I: 2D Depth-Averaged Flow Modeling with an Unstructured Hybrid Mesh (Lai 2010)

The measured and predicted velocity magnitude comparisons at all measurement points are made for both the Sandy River and Columbia River. The comparison of Sandy River is shown below. The agreement between the model and measured data are reasonable.

Conclusion

Dr. Lai's numerical method is well suited to natural river flows with a combination of main channels, side channels, bars, floodplains, and in-stream structures.

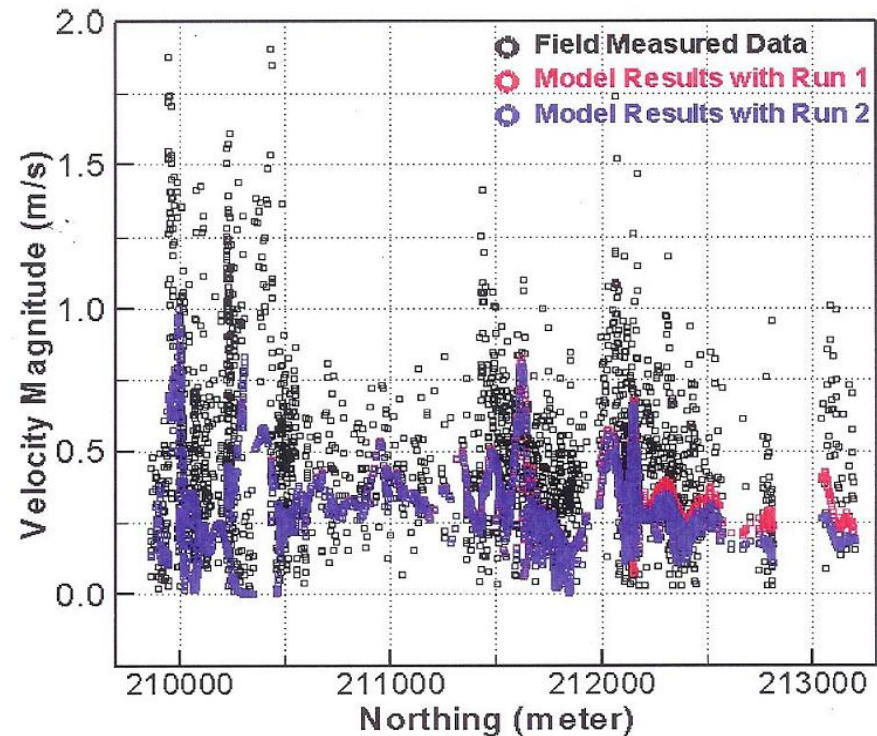


Figure 6 Comparison of field measured and model predicted depth-averaged velocity for the October 12, 2005 flow conditions along the Sandy River (after Dr. Lai)

Case Study II: Analysis of Sediment Transport Following Removal of the Sandy River Delta Dam (Lai 2010)

Sediment Transport Equations

The sediment is assumed to be non-cohesive and non-uniform and is divided into a number of sediment size classes. One has non-equilibrium sediment transport equation for each size class k below.

$$\frac{\partial(hC_k)}{\partial t} + \frac{\partial(hUC_k)}{\partial x} + \frac{\partial(hVC_k)}{\partial y} = \beta\omega_{sk}(C_k^* - C_k)$$

$$C_k^* = q_{sk}/q$$

$$\frac{q_{sk}g(s-1)}{(\tau_b/\rho)^{1.5}} = p_k G(\phi_k)$$

$$s = \frac{\rho_s}{\rho}$$

Shield's parameter of sediment size class k

$$\theta_k = \frac{\tau_b}{\rho g(s-1)d_k}$$

$$\phi_k = \frac{\theta_k}{\theta_c} \left(\frac{d_k}{d_{50}}\right)^\alpha$$

Case Study II: Analysis of Sediment Transport Following Removal of the Sandy River Delta Dam (Lai 2010)

$$G = \begin{cases} 11.933(1 - 0.853/\phi)^{4.5}, & \phi > 1.59 \\ 0.002\exp[14.2(\phi - 1) - 9.28(\phi - 1)^2], & 1.0 \leq \phi \leq 1.59 \\ 0.00218\phi^{14.2}, & \phi < 1.0 \end{cases}$$

$$(1 - p_b) \left(\frac{\partial z_b}{\partial t} \right)_k = -\beta \omega_{sk} (C_k^* - C_k)$$

$$p_{ak} \frac{\partial \delta_a}{\partial t} = \left(\frac{\partial z_b}{\partial t} \right)_k + p_{ak}^* \left(\frac{\partial \delta_a}{\partial t} - \frac{\partial \delta_b}{\partial t} \right)$$

$$p_{ak}^* = p_{ak} \text{ if } \left(\frac{\partial \delta_a}{\partial t} - \frac{\partial z_b}{\partial t} \right) < 0$$

$$p_{ak}^* = \begin{cases} p_{ak} & \text{if } \left(\frac{\partial \delta_a}{\partial t} - \frac{\partial z_b}{\partial t} \right) < 0 \\ \text{sub - surface fraction of sediment size class k} & \text{if } \left(\frac{\partial \delta_a}{\partial t} - \frac{\partial z_b}{\partial t} \right) > 0 \end{cases}$$

$$\frac{\partial z_b}{\partial t} = \sum_k \left(\frac{\partial z_b}{\partial t} \right)_k$$

where h = water depth, C_k = depth-averaged volume sediment concentration for k th sediment size, ω_{sk} = settling velocity of k th sediment size class, β = non-equilibrium adaptation coefficient (by default, 1,0 if net erosion and 0.25 if net deposition), C_k^* = fractional sediment transport capacity for the k th size class, q_{sk} = volumetric sediment transport rate per unit width; p_k = volumetric fraction of the k th sediment size class in the bed; ρ , ρ_s = water and sediment density, respectively; g = gravitational acceleration; τ_b = bed shear stress; θ_c = critical Shield's parameter, 0.04 used in Dr. Lai's project; d_k = diameter of sediment size class k ; d_{50} = median diameter of sediment mixture in bed; α = exposure factor to account for reduction in critical shear stress for larger particles and increase in critical shear stress for smaller particles, 0.65 used in Dr. Lai's project; p_b = bed material porosity; δ_a = thickness of the active layer; p_{ak} = active layer volumetric fraction of sediment size class k

Case Study II: Analysis of Sediment Transport Following Removal of the Sandy River Delta Dam (Lai 2010)

The erosion and deposition pattern may be simulated with accuracy and presented for the 2-year flood existing condition scenario below.

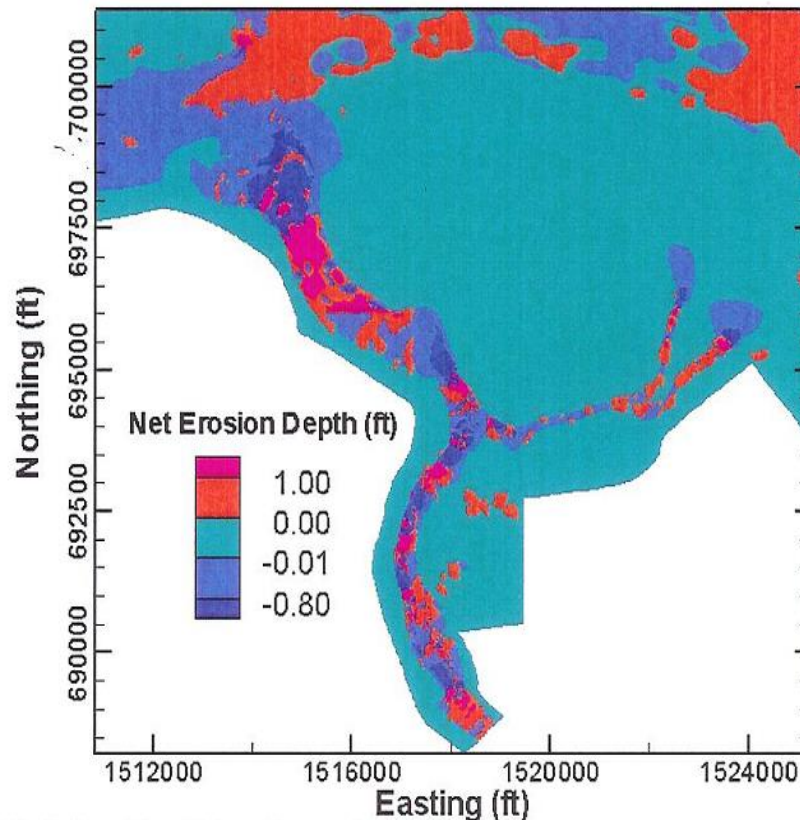
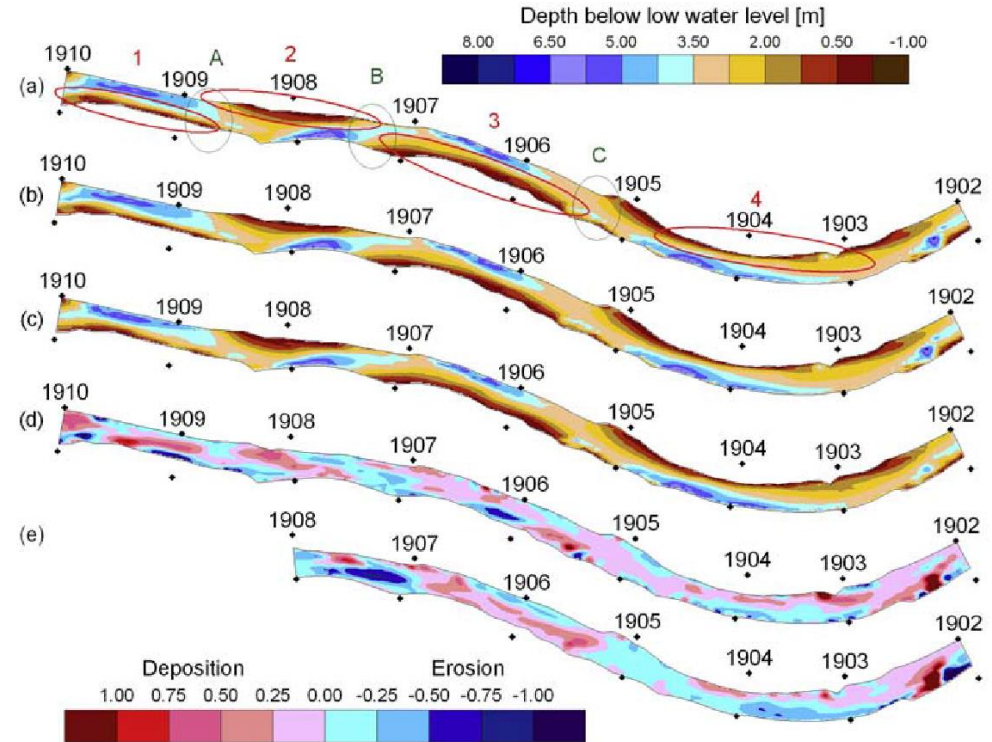


Figure 7 Predicted erosion and deposition pattern 24 hours after a 2-year Sandy River flood (after Dr. Lai)

Case Study III: Three-dimensional CFD modeling of morphological bed changes in the Danube River (Fischer-Antze et al. 2008)

Bed changes in a section of the Danube river for before and after the flood of 2002

Purpose: To investigate the possibility of modeling the bed-changes in a natural river using a 3-D numerical model for prediction of effects of floods or alterations of the physical characteristics of the river



Measured water depths before (b) and after (c) the flood. Measured (d) and computed (e) elevation changes. (a) identifies special regions further discussed in the paper

Case Study III: Three-dimensional CFD modeling of morphological bed changes in the Danube River (Fischer-Antze et al. 2008)

Model type: Full 3D CFD model

Equations:

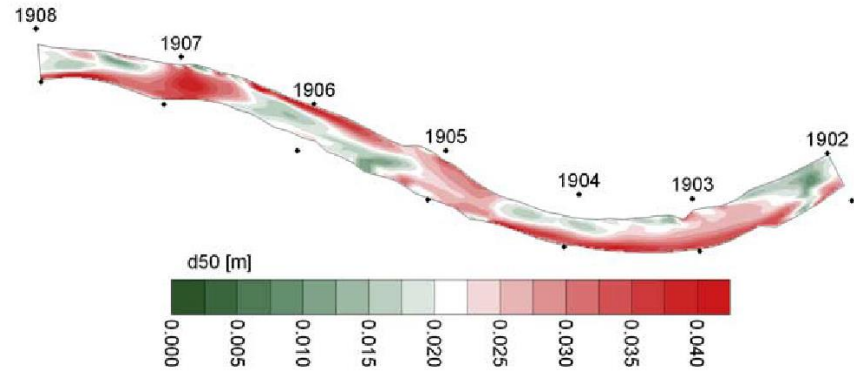
Navier Stokes Equations using the k-epsilon turbulence closure

Nonuniform sediment rating curve from Wu et al. (2000)

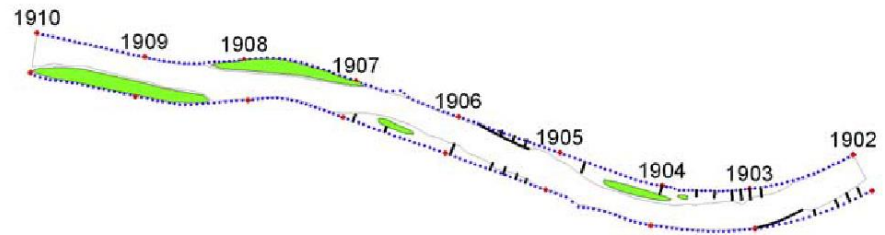
Width-to-depth ratio: 60

Depth-to-grain size ratio: 200

Mean grain size, $d_m = 26$ mm



Median grain size, d_{50} at the end of the computation



Groynes and vegetated areas (green)

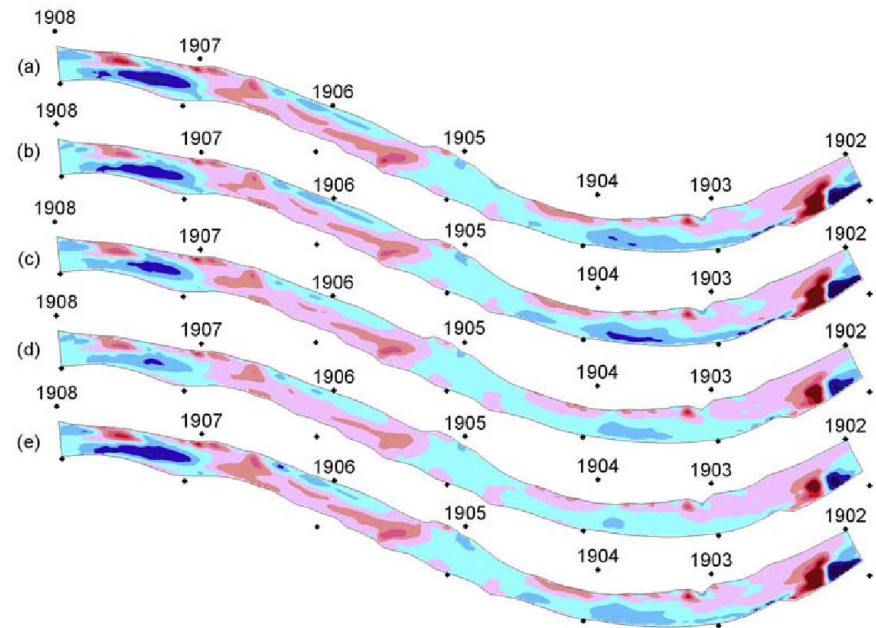
Case Study III: Three-dimensional CFD modeling of morphological bed changes in the Danube River (Fischer-Antze et al. 2008)

Parameter Sensitivity Analysis:

- Varying grid resolution
- Varying time step
- Varying sediment transport parameters

Conclusions:

“CFD model performed well when compared with field measurements. Model was able to represent morphodynamic process, such as deposition processes of a bar and related erosion processes at the scour on the opposite side”



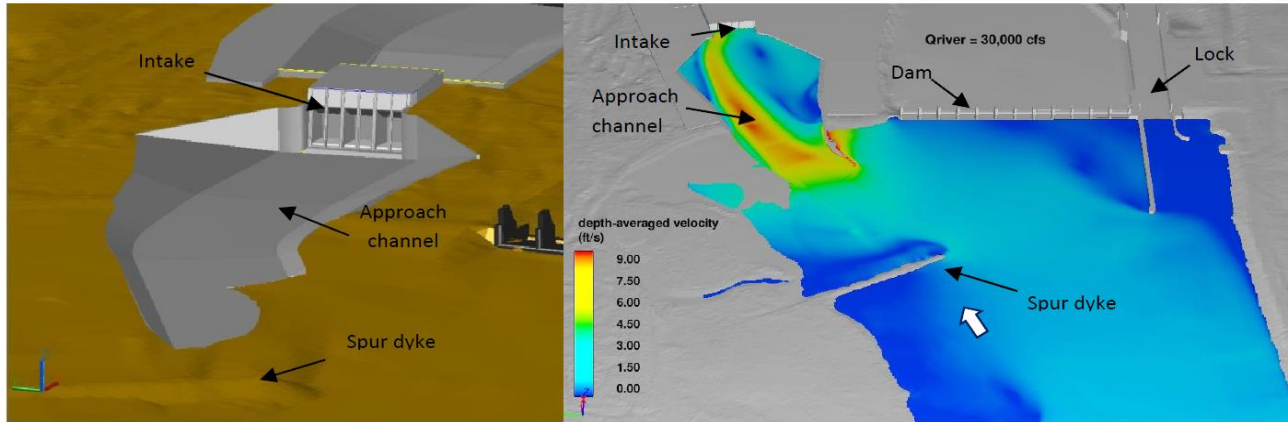
Calculated bed changes, reference calculations with Strickler bed roughness:

- (a) $k_s=0.12$ m
- (b) $k_s=0.2$ m
- (c) $k_s=0.075$ m
- (d) $k_s=2d_{50}$
- (e) $k_s=4d_{50}$

Case Study IV: CFD Modeling of Run-of-River Intakes (Vasquez et al.)

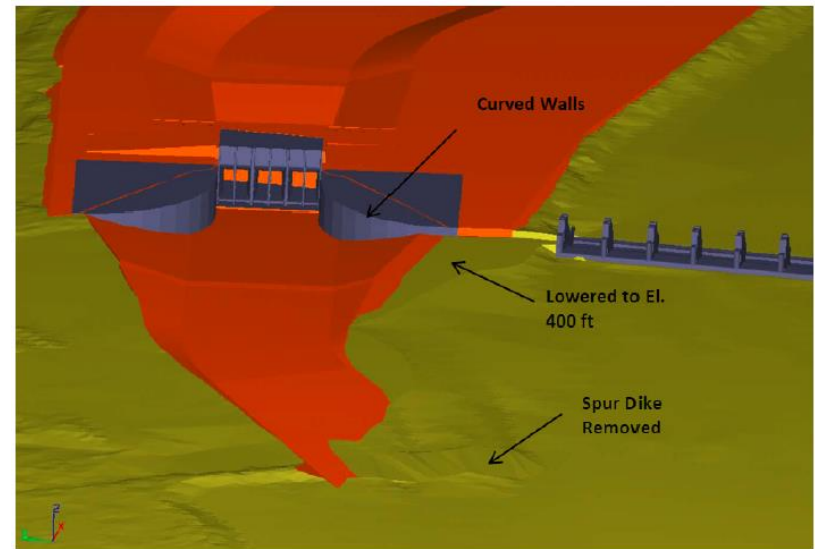
- ▶ Environmental concerns led to increase run-of-river intakes for hydroelectric projects, replacing conventional deep reservoir intakes.
- ▶ Run-of-river intakes have higher approach flow velocities and turbulence, leading to increased sediment inflow at intake.
- ▶ Purpose:
 - Utilize CFD to evaluate potential construction cost savings by reducing excavation downstream from the powerhouse and spillway and potential impact on flow hydraulics.
 - Analyze different intake layouts to minimize head losses and provide more uniform velocity distribution at the intake
 - Assess potential of sediment into intake

Case Study IV: CFD Modeling of Run-of-River Intakes (Vasquez et al.)



Powerhouse intake layout design

- ▶ Flow conditions are highly non-uniform
- ▶ Large eddy in the approach channel contributed to head losses
- ▶ Spur dyke caused uneven flow distribution
- ▶ Optimized layout:
 - Flow of intake moved farther upstream, curved guiding walls, spur dyke removed, lowered invert elevation along the right size of the approach channel entrance

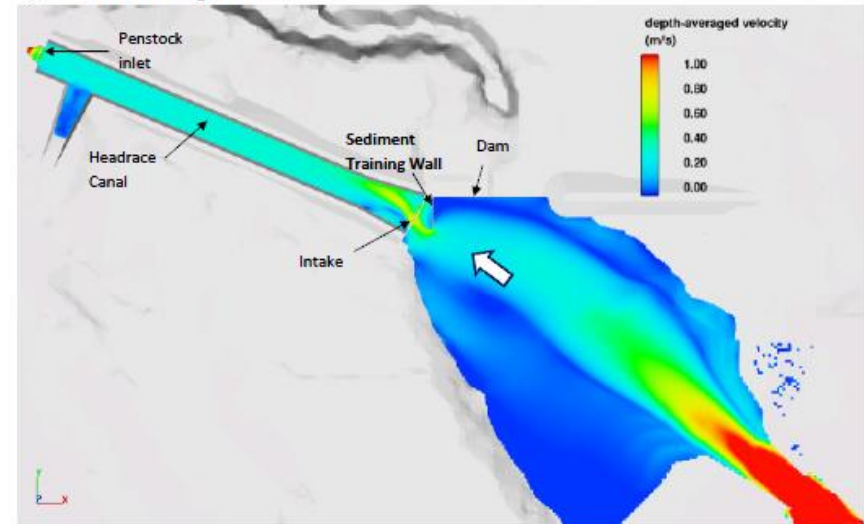


Case Study IV: CFD Modeling of Run-of-River Intakes (Vasquez et al.)

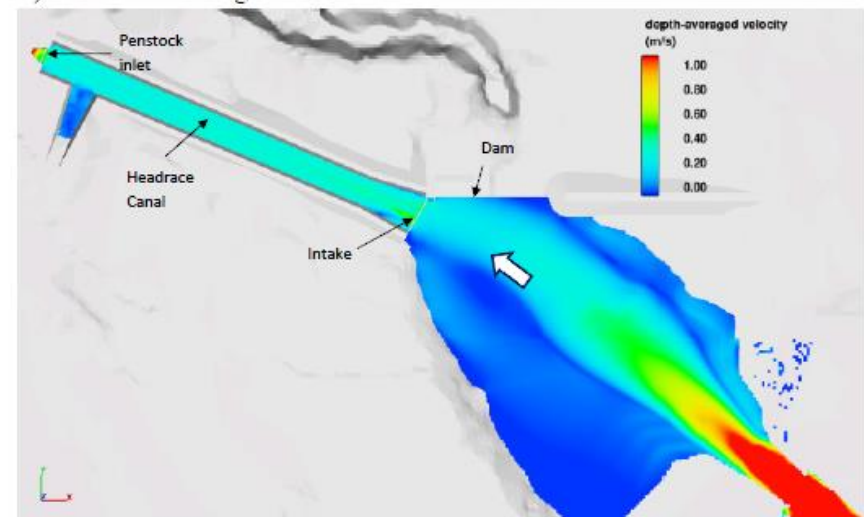
Hydraulics of sediment training wall

- ▶ Usually a training wall is parallel to approach flow direction to increase flushing efficiency. But in this case the the approach flow is almost parallel to the dam, attacking the training wall at at acute angle
- ▶ CFD showed that the training wall caused very turbulent flow conditions with increased local velocities
- ▶ As a result, no training wall was included in the design

a) With training wall



b) Without training wall



Conclusion

- ▶ With the advance of computing technology, numerical simulations using CFD is proven to be useful tool in hydraulic engineering
 - ▶ CFD is viable, and more cost-effective complement, if-not-alternative to physical modeling
- 

References

- ▶ Fischer–Antze, T., N.R.B. Olsen, and D. Gutknecht (2008), Three–dimensional CFD modeling of morphological bed changes in the Danube River, *Water Resources Research* 44, W09422, DOI: 10.1029/2007WR006402
- ▶ Jose Vasquez, Hurtig, K., Hughes, B., (accessed on 2016), *Computational Fluid Dynamics (CFD) Modeling of Run–of–River Intakes*, Northwest Hydraulic Consultatns Ltd., North Vancouver, Canada
- ▶ Weiming Wu, Sam S.Y. Wang, Tafei Jia (2000) Nonuniform sediment transport in alluvial rivers, *Journal of Hydraulic Research*, 38:6, 427–434, DOI: 10.1080/00221680009498296
- ▶ Yong G. Lai, 2010, 2D Depth–Averaged Flow Modeling with an Unstructured Hybrid Mesh, *Journal of Hydraulic Engineering*, 136(1), pp 12–23
- ▶ Yong G. Lai. 2006, *Analysis of Sediment Transport Following Removal of the Sandy River Delta Dam*, US Bureau of Reclamation